Propagation limits of cellular detonation in narrow channels

Brian Devine*, Thomas Westenhofer, Xian Shi
Department of Mechanical and Aerospace Engineering, University of California, Irvine
Irvine, California, United States

1 Introduction

The propagation limits of cellular detonation are governed by two distinct yet related processes. The first process involves losses, such as heat and momentum losses to boundaries or effective flow divergence caused by boundary layer formation downstream of the shock [1–5]. When these cumulative losses surpass a critical threshold and lead to a significant overall velocity deficit, detonation can no longer propagate. This type of limit may be predicted in a one-dimensional (1D) framework [4, 6, 7], similar to how flammability limits are analyzed. The second process concerns the geometric accommodation of the cellular structures within the confining geometry. Detonation propagation fails when the cellular length scale exceeds the confinement dimensions. While the cellular length scale is primarily dictated by the chemical kinetic properties of the mixture, it can also be influenced by losses [5, 8, 9]. We refer to these two processes as the thermodynamic limiting process, related to losses, and the kinetic limiting process, associated with cell geometric accommodation, respectively.

Identifying the dominant failure mechanism is essential for applications such as engine design and accident prevention. If failure is caused by the inability to accommodate cellular structures (i.e., kinetically limited), modifying the confinement may extend detonation limits. The kinetic limit has been observed in the forms of single-headed spinning and zig-zag propagation modes [1, 2, 10], with empirical correlations defining minimum tube diameters [11, 12]. Ozone doping has further demonstrated that by reducing detonation cell sizes, detonation limits can be extended under certain conditions [5, 13]. In contrast, the thermodynamic limiting process remains less explored. Theoretically, a critical failure threshold can be predicted from velocity deficit characteristics due to losses [6, 7], but experimental validation in multidimensional detonations is limited. Loss-induced increases in cell size and eventual detonation failure have been observed, but whether this process alone can dictate detonation limits remains uncertain [3].

This study isolates these processes using narrow-channel experiments with variable geometries and ozone doping. Our objectives are to: (1) demonstrate kinetic limits in narrow channels and explore both geometric and chemical means to modify such limits; (2) assess thermodynamic limits and validate predictive 1D model predictions; and (3) develop a general framework for the propagation limits for cellular detonations. We focus on detonations with regular cellular structures, excluding unsteady limit behaviors such as galloping detonations.

Correspondence to: bdevine@uci.edu

2 Methodology

2.1 Narrow-channel experiments with variable heights and widths

Experiments were conducted in a high-aspect-ratio rectangular channel composed of a stainless steel driver and an aluminum test section. The channel had an inner cross-section of 190.5 mm by 19.05 mm. The driver section (1.68 m) contained a spark ignition source and perforated plates for deflagration-to-detonation transition (DDT), while the test section (3.37 m) included solid aluminum blocks and an optical block near the end. Stoichiometric hydrogen-oxygen mixtures with 80% argon were tested at initial pressures ranging from 5 to 50 kPa. Ozone was introduced via an inline corona discharge generator and fed with the oxygen supply. The channel was evacuated below 400 Pa before filling, and ignition occurred within 15 seconds to prevent ozone decomposition. For near-limit cases, a more reactive ethylene-oxygen mixture ($\sim$1 kPa) was added to assist detonation initiation. Detonation velocities were determined from time-of-arrival data recorded by twelve piezoelectric pressure transducers (PCB 113B22) distributed along the channel. High-speed Schlieren imaging with a Photron Fastcam SA-Z camera was used to capture transient detonation front structures.

Experiments were performed in four configurations: (1) a base channel, (2) the base channel with ozonated mixtures, (3) a half-height channel, and (4) a half-width channel. These configurations were purposely chosen to leverage the unique geometric advantages of a high-aspect-ratio rectangular channel. In these channels, losses are governed by relative surface area, which can be characterized by the hydraulic diameter D_H. For a rectangular channel with height H and width w, the hydraulic diameter is given by:

$$D_H = \frac{4A}{P} = \frac{4Hw}{2(H+w)} = \frac{2Hw}{H+w} \tag{1}$$

In the limit of high aspect ratios, the hydraulic diameter asymptotes to:

$$\lim_{H>>w} D_H = \lim_{H>>w} \frac{2Hw}{H+w} = 2w. \tag{2}$$

This demonstrates that in high-aspect-ratio channels, boundary losses are primarily dictated by the width w, while the height H controls the length scale of cellular accommodation. Therefore, independently varying the channel width or height influenced either the thermodynamic or kinetic limiting process without affecting the other. The half-height channel restricts cell accommodation, affecting the kinetic limit, while the half-width channel amplifies losses, affecting the thermodynamic limit. Ozone doping decreases the cell size of the original mixture, effectively allowing more cells to fit within a given channel. Channel modifications were achieved using machined plastic inserts.

2.2 Modified ZND model with flow divergence

A modified Zeldovich-von Neumann-Döring (ZND) model incorporating flow divergence was implemented to calculate velocity deficit and compare it with experimental measurements. The model accounts for the effects of viscous boundary layers forming along the channel walls, which act as a mass sink to the central flow. Following the approach outlined in [6,14], a flow divergence term, parameterized by a constant K, was added to the conservation equations. The numerical implementation was achieved by modifying the standard ZND model within the Shock and Detonation Toolbox [15] in Cantera [16]. The K values were selected based on the best fit to experimental data to capture the effects of varying channel geometries. The empirical nature of these values does not impact the conclusions of this study. Future work will explore physics-based determinations of K as proposed in recent studies [17, 18].

3 Results and Analysis

In the base, ozone-doped, and half-height channels, detonation failure was dictated by the kinetic limit, where cellular structures became too large to fit within the channel height. As shown in Fig. 1a, for the base channel tests, decreasing initial pressure led to increasing velocity deficits, eventually leading to the characteristic half-cell, zig-zag failure mode at the detonation limit around 9 kPa. Tests with ozone doping reduced cell size and achieved an extension of the detonation limit to a lower pressure at 6 kPa, whereas the half-height channel configuration restricted cell accommodation, causing detonation failure at a higher pressure of 13 kPa. At the limit within each of the three configurations, the half-cell, zig-zag propagation was observed, as shown in Figs. 1b, c, and d. Representative local velocity profiles along the channel of a propagation far away from the limit and a near-limit propagation are shown in Figs. 1e and f, demonstrating the decreasing trend of averaged velocity shown in Fig. 1a. The consistent velocity trends and limiting behaviors across these configurations confirm that detonation failure was governed by cell accommodation constraints and therefore kinetically controlled.

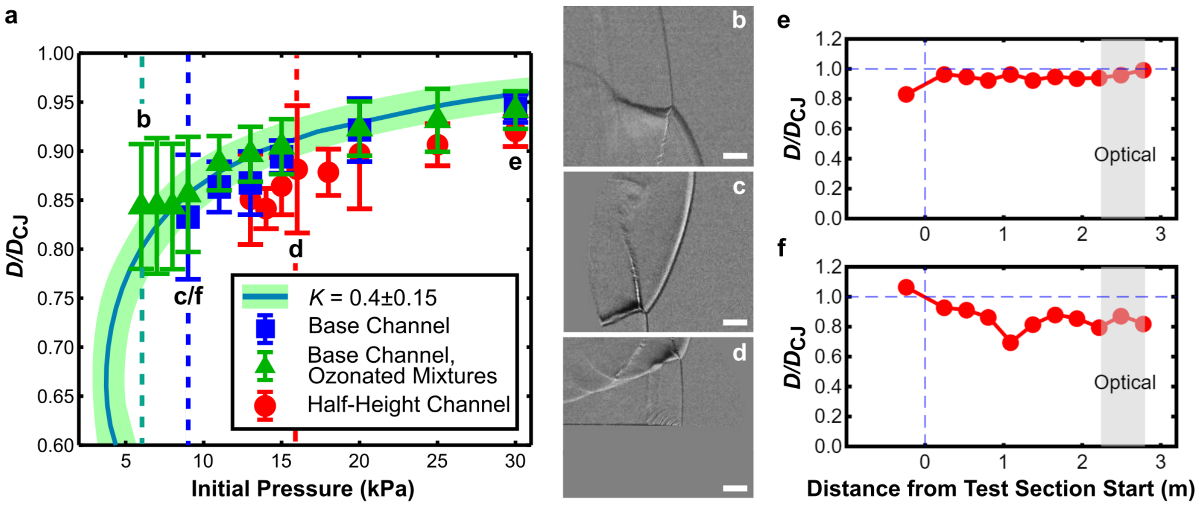

Figure 1: Detonation failures for kinetically-altered mixtures: **a** normalized global average velocity versus initial pressure across the base channel tests and the two kinetically altering configurations. Images **b**, **c**, and **d** display the characteristic zig-zag behavior at the limit for each configuration. Snapshot **d** is scaled to half the size of **b** and **c** to convey the visual effect of the half-height channel. **e** normalized local velocity from the base channel test at 30 kPa. **f** normalized local velocity from the base channel test at 9 kPa. Scale bar in **b** and **c**: 10 mm. Scale bar in **d**: 20 mm.

In contrast, experiments in the half-width channel, shown in Fig. 2, revealed a fundamentally different detonation failure mechanism. Here, failure occurred probabilistically between 35 kPa and 20 kPa, with absolute failure at 20 kPa. Unlike the kinetic limit cases, successful detonations in the half-width channel maintained multi-cell structures throughout the tested initial pressures and even near the failure threshold, as seen in Figs. 2b-d. Unsuccessful detonations, on the other hand, exhibit abrupt failure behavior without transitioning to a zig-zag propagation mode. The statistical analysis of success and failure probabilities in Fig. 2e further supports the presence of a thermodynamic limit, which contrasts with the well-defined kinetic limit observed in previous configurations.

The modified ZND model incorporating flow divergence effectively captured the experimental trends and further provided corroborating evidence on the existence of both limits. For the kinetic limiting cases shown in Fig. 1a, the model, displayed by the green shaded region, showed that detonation failure was still distant from the theoretical turning point, confirming a geometric, kinetic constraint. In contrast,

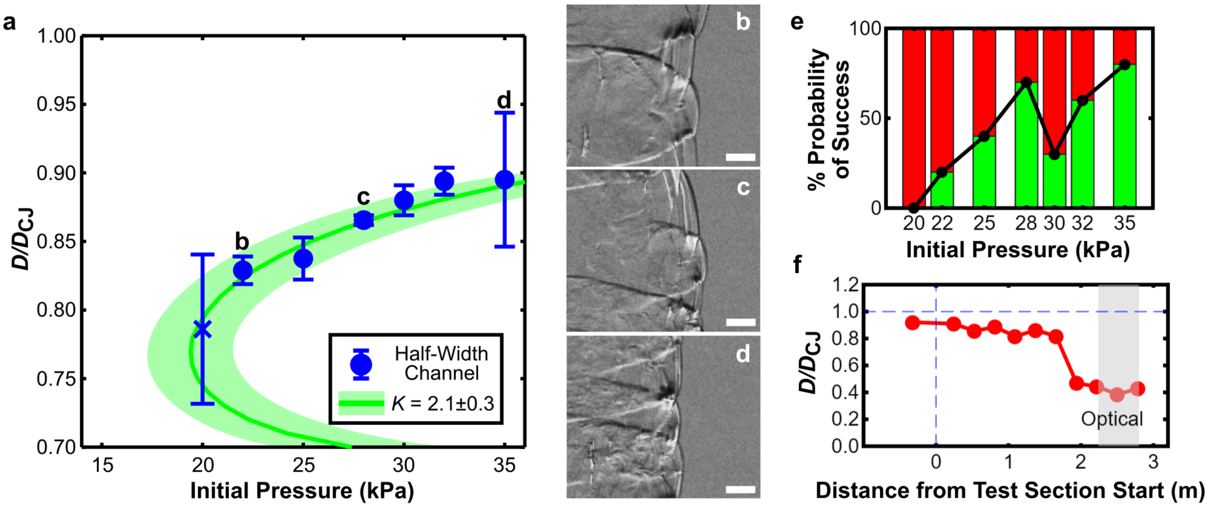

Figure 2: Detonation failures in the half-width channel configuration: **a** normalized global average velocity versus initial pressure with both experimental results and numerical predictions presented. **b**, **c**, and **d** snapshots showing multi-cellular propagation. **e** the likelihood of successful detonation propagation as a function of initial pressure. **f** an example local velocity profile during detonation failure. Scale bar in **b**, **c**, and **d**: 10 mm.

for the thermodynamic limit case shown in Fig. 2a, the experimental failure threshold closely aligned with the model's turning point, suggesting that detonation failure could indeed be caused by losses and that the propagation is thermodynamically constrained.

These findings provide strong evidence that detonation failure in confined systems can be governed by either kinetic or thermodynamic constraints, depending on the specific mixture and boundary conditions. The identification of a thermodynamic limit in cellular detonations is particularly significant, as it implies that propagation failure can occur even when cellular structures remain accommodated within the confinement. This has important implications for detonation-based propulsion and safety applications, where loss-induced failure mechanisms must be considered alongside traditional kinetic constraints.

4 Work In Progress

We are currently exploring additional geometric constraints, extending the framework to irregular mixtures, and improving predictive modeling. The list below provides a summary of our current efforts.

1. To assess whether additional geometric modifications can further promote or restrict detonation propagation, we plan to introduce discrete obstacles in the base channel. These structures may act as kinetic limit enhancers by providing additional surfaces for wave reflection. This exploration will help identify specific boundary features that either enhance or hinder cellular detonation propagation.

2. Our current study focuses on well-defined cellular detonations, but many practical mixtures are composed of lean or hydrocarbon fuels. These mixtures exhibit fundamentally different dynamics, e.g., irregular cellular structures and unsteady propagation near the limit. Future work will explore alternative metrics, such as velocity fluctuations and front curvature, to extend our kinetic limit framework to irregular mixtures.

3. The modified ZND model has successfully captured velocity deficits and limits, but the flow divergence parameter K remains empirically fitted. Incorporating physics-based determinations of K proposed and tested in recent studies [17, 18] will improve predictive accuracy and provide a more complete theoretical framework for thermodynamic limits predicted by the 1D model.

5 Acknowledgments

This research was funded by the Air Force Office of Scientific Research under Grant FA9550-23-1-0185 managed by Dr. Chiping Li and the National Science Foundation Graduate Research Fellowship under Award No. DGE-2235784 to BD.

References

[1] K. Ishii, K. Itoh, and T. Tsuboi, "A study on velocity deficits of detonation waves in narrow gaps," *Proceedings of the Combustion Institute*, vol. 29, no. 2, pp. 2789–2794, 2002.

[2] S. Kitano, M. Fukao, A. Susa, N. Tsuboi, A. Hayashi, and M. Koshi, "Spinning detonation and velocity deficit in small diameter tubes," *Proceedings of the Combustion Institute*, vol. 32, no. 2, pp. 2355–2362, 2009.

[3] J. H. Lee, A. Jesuthasan, and H. D. Ng, "Near limit behavior of the detonation velocity," *Proceedings of the Combustion Institute*, vol. 34, no. 2, pp. 1957–1963, 2013.

[4] M. I. Radulescu and B. Borzou, "Dynamics of detonations with a constant mean flow divergence," *Journal of Fluid Mechanics*, vol. 845, pp. 346–377, 2018.

[5] X. Shi, J. Crane, and H. Wang, "Detonation and its limit in small tubes with ozone sensitization," *Proceedings of the Combustion Institute*, vol. 38, no. 3, pp. 3547–3554, 2021.

[6] Q. Xiao and M. I. Radulescu, "Dynamics of hydrogen–oxygen–argon cellular detonations with a constant mean lateral strain rate," *Combustion and Flame*, vol. 215, pp. 437–457, 2020.

[7] F. Veiga-López, L. Faria, and J. Melguizo-Gavilanes, "Heat and momentum losses in h 2–o 2–n 2/ar detonations: on the existence of set-valued solutions with detailed thermochemistry," *Shock Waves*, pp. 1–11, 2024.

[8] J. H. Lee, "Dynamic parameters of gaseous detonations," *Annual Review of Fluid Mechanics*, vol. 16, pp. 311–336, 1984.

[9] Q. Xiao, A. Sow, B. M. Maxwell, and M. I. Radulescu, "Effect of boundary layer losses on 2d detonation cellular structures," *Proceedings of the Combustion Institute*, vol. 38, no. 3, pp. 3641–3649, 2021.

[10] Y. Gao, H. D. Ng, and J. H. Lee, "Near-limit propagation of gaseous detonations in narrow annular channels," *Shock Waves*, vol. 27, pp. 199–207, 2017.

[11] G. Agafonov and S. M. Frolov, "Computation of the detonation limits in gaseous hydrogen-containing mixtures," *Combustion, Explosion and Shock Waves*, vol. 30, no. 1, pp. 91–100, 1994.

[12] Y. Gao, H. D. Ng, and J. H. Lee, "Minimum tube diameters for steady propagation of gaseous detonations," *Shock Waves*, vol. 24, no. 4, pp. 447–454, 2014.

[13] J. Crane, X. Shi, A. V. Singh, Y. Tao, and H. Wang, "Isolating the effect of induction length on detonation structure: Hydrogen–oxygen detonation promoted by ozone," *Combustion and Flame*, vol. 200, pp. 44–52, 2019.

[14] R. Klein, J. C. Krok, and J. Shepherd, "Curved quasi-steady detonations: Asymptotic analysis and detailed chemical kinetics," GALCIT, California Institute of Technology, Tech. Rep., 1995.

[15] S. T. Browne, J. L. Ziegler, N. P. Bitter, B. E. Schmidt, J. Lawson, and J. E. Shepherd, "Sdtoolbox: Numerical solution methods for shock and detonation jump conditions," 2001. [Online]. Available: https://shepherd.caltech.edu/EDL/PublicResources/sdt/

[16] D. G. Goodwin, R. L. Speth, H. K. Moffat, and B. W. Weber, "Cantera: An object-oriented software toolkit for chemical kinetics, thermodynamics, and transport processes," 2018, version 2.4.0. [Online]. Available: https://www.cantera.org

[17] J. Smith, C. Schmitt, Q. Xiao, and B. Maxwell, "On the nature of transverse waves in marginal hydrogen detonation simulations using boundary layer loss modeling and detailed chemistry," *Combustion and Flame*, vol. 268, p. 113598, 2024.

[18] F. Zangene and M. I. Radulescu, "Role of the argon and helium bath gases on the structure of h2/o2 detonations," *arXiv preprint arXiv:2410.17561*, 2024.